16th World Conference on Earthquake, 16WCEE 2017

Santiago Chile, January 9th to 13th 2017

Paper N° 939

Registration Code: S-L1461939050

LIFE-CYCLE RESILIENCE OF DETERIORATING BRIDGE NETWORKS UNDER EARTHQUAKE SCENARIOS

F. Biondini[(1)], L. Capacci[(2)], A. Titi[(3)]

[(1)] *Professor, Department of Civil and Environmental Engineering, Politecnico di Milano, fabio.biondini@polimi.it*
[(2)] *Ph.D. Student, Department of Civil and Environmental Engineering, Politecnico di Milano, luca.capacci@polimi.it*
[(3)] *Postdoc Research Associate, Department of Civil and Environmental Engineering, Politecnico di Milano, andrea.titi@polimi.it*

Abstract

Resilience of bridges and infrastructure networks is generally investigated considering damage and disruption caused by sudden extreme events, such as earthquakes. However, damage could also arise continuously in time due to aging and structural deterioration, which can modify over time the structural performance and functionality and, consequently, the system resilience. Therefore, for critical infrastructures exposed to seismic and environmental hazards, resilience depends on the time of occurrence of the seismic event. This paper investigates the life-cycle seismic resilience of aging infrastructures and presents a probabilistic approach to seismic assessment of deteriorating bridges and resilience analysis of road networks under prescribed earthquake scenarios. The time-variant seismic fragilities of the deteriorating bridges in the network are assessed for several limit states, from damage limitation up to collapse. The seismic demand is evaluated for each bridge based on a ground motion prediction equation in terms of earthquake magnitude and epicentral distance. The corresponding levels of seismic damage are derived from the time-variant fragilities and related to vehicle restrictions and traffic limitations. A traffic analysis is carried out over the entire road network to compute both the time-variant system functionality and life-cycle seismic resilience under prescribed post-event recovery processes. The proposed approach is applied to reinforced concrete bridges in a highway network with detour and re-entry link. The bridges are exposed to chloride-induced corrosion and earthquake scenarios considering different magnitude and epicenter location. The results show the detrimental effects of aging and structural deterioration and emphasize the role of the earthquake scenario on the time-variant seismic performance of bridge structures and life-cycle resilience of road networks.

Keywords: Seismic resilience; system functionality; road networks; aging bridges; corrosion; life-cycle performance.

1. Introduction

A proper management of strategic structures and infrastructure facilities, such as highway bridges, is essential to prevent or minimize outages and disruptions after seismic events [1-3]. In fact, road infrastructure networks are of primary importance in the post-event emergency phase in order to ensure both a quick deployment of aids and resources to distressed communities and a prompt repair of the surrounding lifelines and buildings [4]. Damage of bridges may affect the network functionality and involve significant economic losses due to repair interventions, traffic delay, and network downtime, among others. Therefore, the definition of effective post-event recovery processes of damaged bridges is a key factor to ensure suitable resilience levels of the entire network [5, 6].

Seismic resilience is becoming a driving concept in design, assessment, monitoring, maintenance and management of structures and infrastructure systems. Resilience can be defined as the capability of a system to withstand the effects of disruptive events and to recover promptly and efficiently the pre-event functionality [7-10]. For bridges and infrastructure networks, this performance indicator is often investigated considering the consequences of the sudden damage induced by seismic events [9-13]. However, for structural systems exposed to seismic and environmental hazards, damage can also arise continuously over time due to the effects of aging and structural deterioration. Consequently, seismic resilience of deteriorating bridges and infrastructure networks depends on the time of occurrence of the seismic event [14-16]. Therefore, system functionality and seismic resilience should be formulated as time-variant performance indicators under a life-cycle perspective to properly support the decision making process for management of critical infrastructures.

This paper presents a life-cycle probabilistic approach to seismic assessment of bridge structures and resilience analysis of road networks considering the interaction of environmental and seismic hazards under prescribed earthquake scenarios. The time-variant seismic fragilities of the deteriorating bridges in the network are assessed for several limit states, from damage limitation up to collapse, through nonlinear incremental dynamic analysis and Monte Carlo simulation. The seismic demand is evaluated for each bridge based on a ground motion prediction equation in terms of earthquake magnitude and epicentral distance. The corresponding levels of seismic damage, which are depending on the time of occurrence of the seismic event because of aging and structural deterioration, are derived from the time-variant fragilities and related to vehicle restrictions and traffic limitations. A traffic analysis is finally carried out over the entire road network to compute the time-variant system functionality and life-cycle seismic resilience under prescribed post-event recovery processes.

The proposed approach is applied to reinforced concrete (RC) bridges in a highway network with detour and re-entry link. The bridges are exposed to chloride-induced corrosion and earthquake scenarios with different magnitude and epicenter location. The objective of the application is to show the detrimental effects of aging and structural deterioration on the seismic performance of bridge structures and seismic resilience of road networks and emphasize the importance of the earthquake scenario in a multi-hazard life-cycle-oriented approach to seismic design of resilient structures and infrastructure systems.

2. Seismic assessment of spatially distributed RC bridges under corrosion

2.1 Incremental dynamic analysis and seismic capacity

In this paper, the seismic capacity of RC bridges is evaluated through nonlinear incremental dynamic analysis [17] by assuming the peak ground acceleration (PGA) as intensity measure and the maximum drift $\theta_{max}=\Delta_{max}/H$, with Δ_{max} = maximum top displacement of a bridge pier and H = pier height, as damage measure. The structural modeling is based on beam finite elements with material non-linearity lumped at the beam ends, where plastic hinges are expected to occur [18]. The nonlinear behavior of the plastic hinges is defined in terms of bending moment M versus curvature χ relationship, according to the constitutive laws of the materials. For concrete, the model proposed by Mander et al. [19] is assumed. For steel, a bilinear elastic-plastic model is adopted. The hysteretic behavior is based on the Takeda model [20], with a backbone curve defined by a stepwise linearization of the moment versus curvature diagram. The length of the plastic hinge is evaluated as proposed by Paulay & Priestley [21].

2.2 Damage limit states and seismic fragility

The damage limit states can be conveniently associated with threshold values of the maximum drift θ_{max}, for example as follows [22]:

- Slight Damage (SD): $\theta_{max}=\theta_y$;
- Moderate Damage (MD): $\theta_{max}=\theta_y+0.3\theta_p$;
- Extensive Damage (ED): $\theta_{max}=\theta_y+0.6\theta_p$;

where $\theta_p=\theta_u-\theta_y$, and θ_y and θ_u are the drift limits associated with, respectively, the first yielding and ultimate curvatures of the bridge piers in the undamaged state. The drifts θ_y and θ_u are computed by nonlinear static (pushover) analysis. In addition, a structural collapse limit state (SC), associated with the loss of dynamic equilibrium under ground motion, is considered.

The seismic capacities of RC bridges under uncertainty are investigated by means of fragility analysis and described in probabilistic terms by fragility curves providing for each damage limit state the probability of exceedance versus the PGA. It is worth noting that seismic capacities and fragility curves are time-variant due to aging and structural deterioration [14-16].

2.3 Effects of reinforcing steel corrosion

The application presented in this paper deals with RC bridges exposed to chloride-induced corrosion [23]. The chloride ingress is modeled by the Fick's laws of diffusion and described by using cellular automata [24, 25].

The main effect of the corrosion process induced by chloride diffusion is a reduction of the cross-sectional area of reinforcing steel bars. This effect can be described by means of a dimensionless damage index δ_s which provides a measure of damage within the range [0,1]. Corrosion may also cause a significant reduction of ductility of the reinforcing steel bars. Moreover, the formation of oxidation products may lead to propagation of longitudinal splitting cracks and concrete cover spalling. These effects are modeled as a reduction of both the ultimate steel strain ε_{su} and concrete strength f_c as a function of the damage index δ_s [26].

The corrosion rate at point $\mathbf{x}$ and time t depends on the chloride concentration $C=C(\mathbf{x}, t)$, and damage initiates once concentration reaches a critical value $C=C_{crit}$. Based on available data for chloride attacks, a linear relationship between corrosion rate and chloride concentration is assumed as follows:

$$\frac{\partial \delta_s(\mathbf{x},t)}{\partial t} = q_s\, C(\mathbf{x},t) \tag{1}$$

where q_s is a damage rate coefficient. Further details on the corrosion model can be found in [24-26].

2.4 Earthquake scenario and seismic demand

For spatially distributed bridges, the earthquake scenario should consider both magnitude and epicentral distances. The following ground motion prediction equation, proposed by Bindi et al. [27] based on the strong motion database for Italy, is considered:

$$\log_{10}\mathrm{PGA} = 3.672 + F_D(d,M) + F_M(M) + F_S + F_{sof} \tag{2}$$

$$F_D(d,M) = [-1.940 + 0.413\,(M - M_{ref})]\log_{10}\frac{\sqrt{d^2+h^2}}{d_{ref}} - 0.000134\left(\sqrt{d^2+h^2} - d_{ref}\right) \tag{3}$$

$$F_M(M) = \begin{cases} -0.262\,(M-M_h) - 0.0707\,(M-M_h)^2 & ,\text{for } M \le M_h \\ 0 & ,\text{otherwise} \end{cases} \tag{4}$$

where PGA is in cm/s^2, $F_D(d,M)$, $F_M(M)$, F_S, and F_{sof} are the distance function, the magnitude scaling, the site amplification, and the style-of-faulting correction, respectively, M is the moment magnitude, d is the epicentral distance (in km), h=10.322 km is a pseudo-depth parameter, d_{ref}=1 km, M_{ref}=5, and M_h=6.75.

3. Seismic resilience of road networks

3.1 Network traffic flow analysis

The performance and functionality of road networks where users take part in the origin/destination flows can be assessed based on traffic flow response and minimum travel time [2]. A road arc is defined by the origin *i*, where the flow gets into the arc, and the destination *j*, where the users get out of the arc. The travel time c_{ij} of the arc *i*–*j* can be expressed as a function of several parameters:

$$c_{ij} = c_{ij}(f_{ij}, \mathbf{p}_{\mathbf{road}}, \mathbf{c}_{\mathbf{road}}) \tag{5}$$

where f_{ij} is the vehicle flow per unit of time in the arc *i*–*j*, $\mathbf{p}_{\mathbf{road}}$ includes road parameters such as arc length L_{ij} and number of lanes n_L, and $\mathbf{c}_{\mathbf{road}}$ is the road class depending on several factors, including the minimum distance $d_{\min}$ between vehicles, the corresponding speed limit, or critical speed v_{cr}, and the maximum speed limit $v_{\max}$. The travel time c_{ij} is related to the traffic flow f_{ij} as follows [2]:

$$c_{ij} = c_{ij}^0 \left[1 + \alpha \left(\frac{f_{ij}}{f_{ij}^{cr}} \right)^{\beta} \right] \tag{6}$$

where $c^0_{ij}=L_{ij}/v_{\max}$ is the travel time at free flow, $f_{ij}^{cr}=n_L(v_{cr}/d_{\min})$ is the practical capacity, α=0.15, and β=4 [28].

The total travel time *TTT*, which is the time spent by all users to reach any destination from any origin departing in a fixed time window, is evaluated as follows [2]:

$$TTT = \sum_{i \in I} \sum_{j \in J} \int_0^{f_{ij}} c_{ij}(f)\, df \tag{7}$$

where *i* and *j* are generic nodes of the network, and *I* and *J* are the whole sets of nodes. The optimal traffic flow distribution is identified by minimizing the total travel time. In this study, initial traffic flows are prescribed a priori. However, traffic flows related to the condition of the network can also be considered [2, 29].

3.2 Type of users and traffic limitations

The type of users of road networks depends on the needs and duties associated with travels. Three different types of traffic flows are considered: light vehicles f_l, heavy vehicles f_h, and emergency vehicles f_e. Restrictions to type of vehicles and limitations to traffic network capacity are applied depending on the damage state of the bridges in the network [30]. The following four traffic limitations, identified by a Decision Variable $DV_b=k$ associated to four bridge damage levels k=1,…,4, are assumed:

– Weight Restriction (DV_b=1): transit of heavy vehicles is forbidden and maximum speed is reduced;
– One Lane Open Only (DV_b=2): only one lane is left open to traffic due to repair activities;
– Emergency Access Only (DV_b=3): transit of emergency vehicles only is allowed;
– Closure (DV_b=4): transit is forbidden to all vehicles.

The traffic limitations are represented as follows:

$$\begin{cases} f_h = 0 \text{ and } \tilde{v}_{\max} < v_{\max} & , DV_b = 1 \\ n_L = 1 & , DV_b = 2 \\ f_l = 0 & , DV_b = 3 \\ f_e = 0 \text{ or } n_L = 0 & , DV_b = 4 \end{cases} \tag{8}$$

where the restriction $DV_b=k$, with k=2,3,4, is inclusive of the traffic limitations associated with $DV_b < k$. In this paper, the bridge damage thresholds are associated with the attainment of the limit states SD, ED, MD, and SC.

3.3 Network functionality and recovery model

The functionality $Q=Q(t)\in[0,1]$ of the road network is defined as follows [3]:

$$Q(t)=\frac{TTT_u}{TTT_d(t)} \tag{9}$$

where TTT_u and $TTT_d=TTT_d(t)$ are the total travel times, respectively, of the undamaged and damaged network at time t. A seismic event that strikes the system at time t_0 may cause a sudden loss of functionality $\Delta Q=\Delta Q(t_0)$ due to vehicle restrictions and traffic limitations imposed to damaged bridges.

The functionality drop ΔQ can be recovered by post-event restoration activities over a recovery time interval $\delta_r = t_f - t_i$, where $t_i = t_0+\delta_i$ and t_f are the initial and final time of the restoration process, respectively, and δ_i is the idle time. The purpose of repairing activities is to restore the pre-event seismic capacity of the bridges in the network. The following recovery model $r=r(t)\in[0,1]$ is adopted at the bridge component level [16, 31]:

$$r(\tau)=\begin{cases}\omega^{1-\rho}\tau^{\rho} & ,0\le\tau\le\omega\\ 1-(1-\omega)^{1-\rho}(1-\tau)^{\rho} & ,\omega<\tau\le 1\end{cases} \tag{10}$$

where $\tau=(t-t_i)/\delta_r\in[0,1]$ is a dimensionless time variable, and $\omega\in[0,1]$ and $\rho\ge0$ are parameters which define the shape of the recovery profile. The values of the shape parameters depend on the damage state to be restored.

The road network functionality is described by a discrete set of values as a function of the damage state of the bridges. Therefore, at the network level a constant stepwise recovery model is achieved [32].

3.4 Network seismic resilience

The seismic resilience R of the road network is computed through the integration of the constant stepwise network functionality recovery function over a time horizon t_h as follows:

$$R(t_0)=\frac{1}{t_h-t_0}\sum\nolimits_{\Delta t_{b,i}} Q_{\Delta t_{b,i}}\Delta t_{b,i} \tag{11}$$

where $Q_{\Delta tb,i}$ is the level of network functionality over the time interval $\Delta t_{b,i}$ between two subsequent steps of the restoration process, which depends on the damage states and corresponding repair activities carried out on the bridges in the network. In this way, resilience can be computed for each potential damage state of the network. An overall measure of resilience versus the seismic demand is achieved by a weighted average of the resilience levels by assuming damage probabilities, i.e. the probabilities of being in a damage state, as weight coefficients.

It is worth noting that the seismic resilience $R=R(t_0)$ is a function of the time of occurrence of the seismic event t_0 due to the combined effects of sudden seismic damage and continuous structural deterioration, which affect both the functionality drop and the recovery profile [15].

4. Illustrative example

4.1 RC box-girder bridge

The four-span continuous RC bridge shown in Fig. 1 is considered [13, 16, 33, 34]. The total length of the bridge deck is 200 m, with spans of 50 m. The height of the bridge piers is 14 m. Fig. 2.a shows the box girder cross-section of the deck. The piers have circular cross-section [35] and are reinforced with 36 steel bars with diameter Ø=30 mm, as shown in Fig. 2.b. Roller supports are assumed at the abutments. The constitutive laws of the materials are defined by the following initial nominal values of the material properties: concrete compression strength f_c=40 MPa; steel yielding strength f_{sy}=450 MPa; concrete ultimate strain in compression ε_{cu}=0.35%; steel ultimate strain ε_{su}=7.5%. Seismic analysis is carried out by considering a uniform gravity load of 315 kN/m, including self-weight, dead loads and a 20% of live loads, applied on the deck.

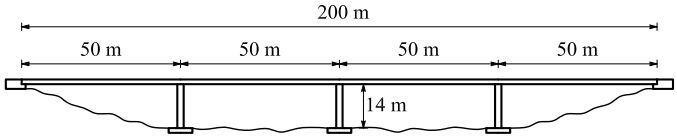

Fig. 1 – Four-span continuous RC box-girder bridge.

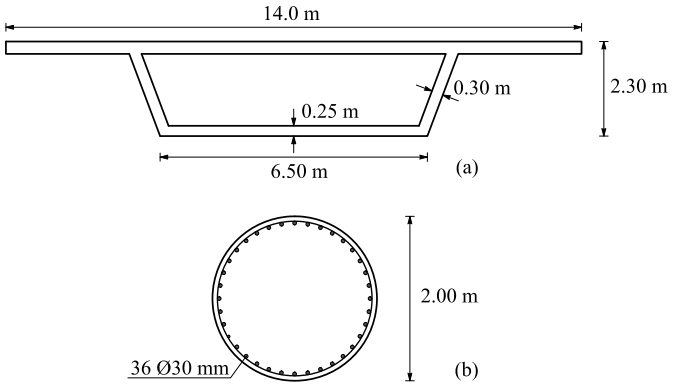

Fig. 2 – RC bridge: (a) deck cross-section; (b) pier cross-section, with reinforcement layout.

The deck is modeled by elastic beam elements, since nonlinear behavior is expected to develop only in the piers. Non-linear time-history dynamic analyses are performed for a set of 10 artificial earthquakes generated to comply with the elastic response spectrum given by Eurocode 8 for soil type B [36, 37].

4.2 Bridge fragility analysis

The piers are exposed to a chloride diffusive attack on the external surface, with nominal concentration C_0=3% [wt.%/c]. A nominal diffusivity coefficient D=15.8×10^{-12} m^2/sec is assumed. The corrosion damage is evaluated by assuming a nominal damage rate coefficient q_s = (0.02 year^{-1})/C_0, with corrosion initiation associated with a nominal critical threshold of concentration C_{crit}=0.6% [wt.%/c].

The uncertainties related to the structural system and the damage process are taken into account in probabilistic terms by assuming the random variables, probability distributions, and coefficients of variation listed in Table 1 [25, 38]. Nominal values are assumed as mean values. Random variables are considered uncorrelated. The seismic fragility analysis is carried out by Monte Carlo simulation based on Latin Hypercube Sampling. Further details about the simulation process can be found in [22].

The results of the probabilistic analysis are shown in Fig. 3 in terms of lognormal fitting of the bridge fragility curves for each limit state over a 100-year lifetime based on a sample of 1000 realizations (100 samples × 10 accelerograms). The vulnerability of the bridge to the SD limit state slightly decreases over time due to the increase of flexibility of the damaged piers in the transition from concrete cracking to steel yielding. For the other limit states, as expected, the probability of exceedance increases over time due to the effects of corrosion.

Table 1 – Probability distributions and coefficients of variation

Random Variable (t = 0)	Distribution	C.o.V.
Concrete strength, f_c	Lognormal	5MPa/$f_{c,\text{nom}}$
Steel strength, f_{sy}	Lognormal	30MPa/$f_{sy,\text{nom}}$
Viscous damping, ξ	Normal (*)	0.40
Diffusivity, D	Normal (*)	0.20
Damage rate, q_s	Normal (*)	0.30
Chloride concentration, C_0	Normal (*)	0.30
Critical concentration, C_{crit}	Beta (**)	0.15

(*) Truncated distribution with non-negative outcomes. (**) Lower bound $b_{\min}$ = 0.2. Upper bound $b_{\max}$ = 2.0.

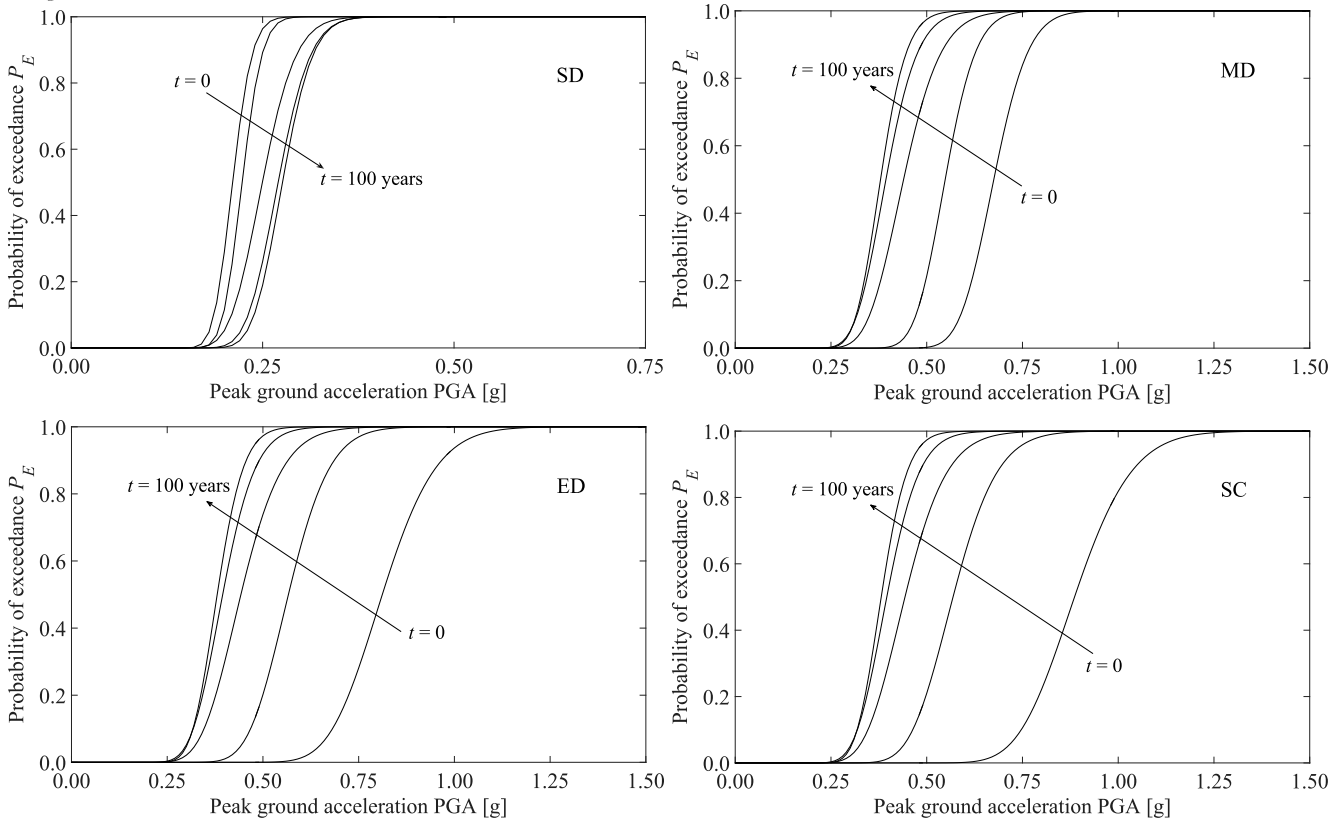

Fig. 3 – Lognormal fitting of the fragility curves of the RC bridge (t = 0, 25, 50, 75, and 100 years).

4.3 Highway network and resilience levels

The highway road network shown in Fig. 4 is considered. The network layout is characterized by one origin and one destination, two bridges B_1 and B_2 located on the main highway in proximity of the origin/destination nodes, and a possible detour route with re-entry link. Table 2 summarizes the traffic parameters of the three types of road segments (main highway, secondary road, re-entry link).

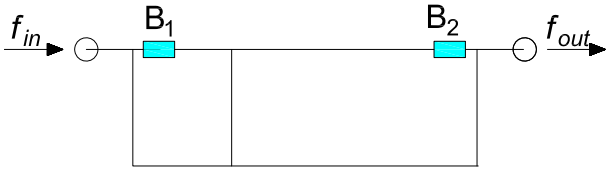

Fig. 4 – Highway network with two bridges, detour route and re-entry link.

Table 2 – Traffic parameters of the road segments.

Traffic Parameters	Highway Road	Secondary Road	Re-entry Link
Length L [km]	10	40	1
No. of lanes n_L	3	2	1
Speed limit v_{max} [km/h]	130	90	90
Lowered speed limit $\tilde{v}_{max}$ [km/h]	70	50	50
Critical speed v_{cr} [km/h]	65	65	65
Minimum distance d_{min} [m/cars]	30	30	30

Traffic restrictions are applied to the bridges depending on their damage state. The loss of network functionality is recovered by post-event bridge repairs, which allow a progressive removal of traffic limitations [13]. The shape parameters ω and ρ of the bridge recovery profiles are selected based on the damage state to be restored. In particular, for each damage state k the recovery process of each bridge leads to restore capacity levels $r_{DS,p}$ at time instants t_p, with p=1,…,k, with stepwise increments of the network functionality over the recovery time interval δ_r. Shape parameters, capacity targets, and recovery time intervals δ_r are listed in Table 3.

The functionality profile is evaluated based on traffic analysis. For a highway network with two bridges and five bridge damage states there are 5^2=25 possible network functionality profiles. The corresponding resilience levels are reported in matrix form in Table 4. The resilience matrix indicates the different importance of the bridges in the network depending on their location. The damage of the bridge that is farthest away from the re-entry link (bridge B_2) is the most critical in terms of network functionality and seismic resilience.

Table 3 – Shape parameters, capacity targets, and recovery time intervals for each bridge damage state.

Damage	ω	ρ	$r_{DS,1}$	$r_{DS,2}$	$r_{DS,3}$	$r_{DS,4}$	δ_r [days]
SD	0.20	2.0	1.00	-	-	-	30
MD	0.40	3.0	0.50	1.00	-	-	90
ED	0.60	4.0	0.20	0.50	1.00	-	180
SC	0.80	5.0	0.05	0.20	0.50	1.00	300

Table 4 – Resilience matrix of the highway network.

Bridge B_2 \ Bridge B_1	No damage	SD	MD	ED	SC
No damage	1.000	0.990	0.958	0.806	0.507
SD	0.978	0.973	0.945	0.806	0.507
MD	0.925	0.921	0.907	0.800	0.506
ED	0.737	0.737	0.736	0.715	0.479
SC	0.380	0.380	0.380	0.376	0.340

4.4 Earthquake scenarios and life-cycle seismic resilience of the highway network

Fig. 5 shows the contour map of the PGA [g] for the moment magnitude M versus epicentral distance d assuming soil type B of Eurocode 8 [37] and reverse faulting, with site amplification F_S=0.162 and style-of-faulting correction F_{sof}=0.105 [27]. For a given magnitude, the bridges B_1 and B_2 are exposed to different seismic demand depending on their epicentral distances. The influence of the earthquake scenario on the time-variant seismic performance of the bridges and life-cycle seismic resilience of the highway network is investigated by varying the earthquake magnitude and considering a grid of potential epicenters with size 5×5 km, as shown in Fig. 6. The corresponding seismic demands for bridges B_1 and B_2 are reported in Table 5.

For the sake of synthesis and to emphasize the importance of the bridge location in the network layout, the fragility curves shown in Fig. 3 are assumed for both bridges B_1 and B_2 without correlation. However, it is worth noting that different and/or correlated fragilities can be easily accommodated in the proposed procedure. Fig. 7 shows the seismic resilience of the highway network, computed as the weighted average of the resilience levels by assuming the damage probabilities as weight coefficients, versus the moment magnitude for the set of epicenter locations shown in Fig. 6 and different times of occurrence of the seismic event over a 100-year lifetime. As expected, resilience decreases as the seismic demand increases and bridge epicentral distances decrease. Moreover, resilience decreases over time due to the detrimental effects of structural deterioration and the impact of the environmental exposure depends on the earthquake scenario and related seismic exposure of the most important bridges in the network. This emphasizes the key role of the earthquake scenario in a multi-hazard life-cycle-oriented approach to seismic design of resilient structures and infrastructure systems.

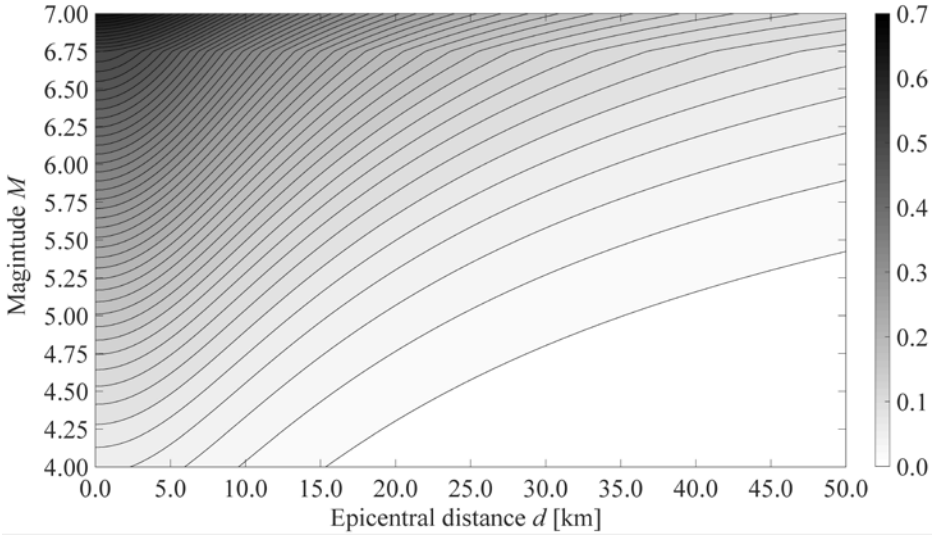

Fig. 5 – Contour map of PGA [g] for magnitude M vs epicentral distance d for soil type B and reverse faulting.

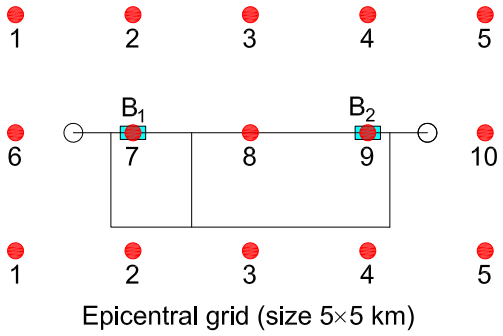

Fig. 6 – Grid of potential epicenters for the earthquake scenarios (grid size 5×5 km).

Table 5 – Seismic demand (PGA [g]) of the bridges B_1 and B_2 under earthquake scenarios defined in terms of moment magnitude and epicenter location: coordinates (x,y) in km, with origin in the bridge B_1 (epicenter #7).

M	Bridge B_1						Bridge B_2					
	#1 (–5,±5)	#2 (0,±5)	#3 (5,±5)	#6 (–5,0)	#7 (0,0)	#8 (5,0)	#1 (–5,±5)	#2 (0,±5)	#3 (5,±5)	#6 (–5,0)	#7 (0,0)	#8 (5,0)
4.0	0.036	0.044	0.036	0.044	0.056	0.044	0.013	0.022	0.036	0.015	0.026	0.044
4.5	0.066	0.080	0.066	0.080	0.100	0.080	0.027	0.044	0.066	0.030	0.049	0.080
5.0	0.115	0.136	0.115	0.136	0.167	0.136	0.052	0.078	0.115	0.055	0.088	0.136
5.5	0.182	0.212	0.182	0.212	0.255	0.212	0.089	0.130	0.182	0.095	0.143	0.212
6.0	0.267	0.305	0.267	0.305	0.359	0.305	0.142	0.198	0.267	0.151	0.216	0.305
6.5	0.361	0.406	0.361	0.406	0.466	0.406	0.210	0.279	0.361	0.220	0.301	0.406
7.0	0.529	0.583	0.529	0.583	0.656	0.583	0.334	0.425	0.529	0.348	0.453	0.583

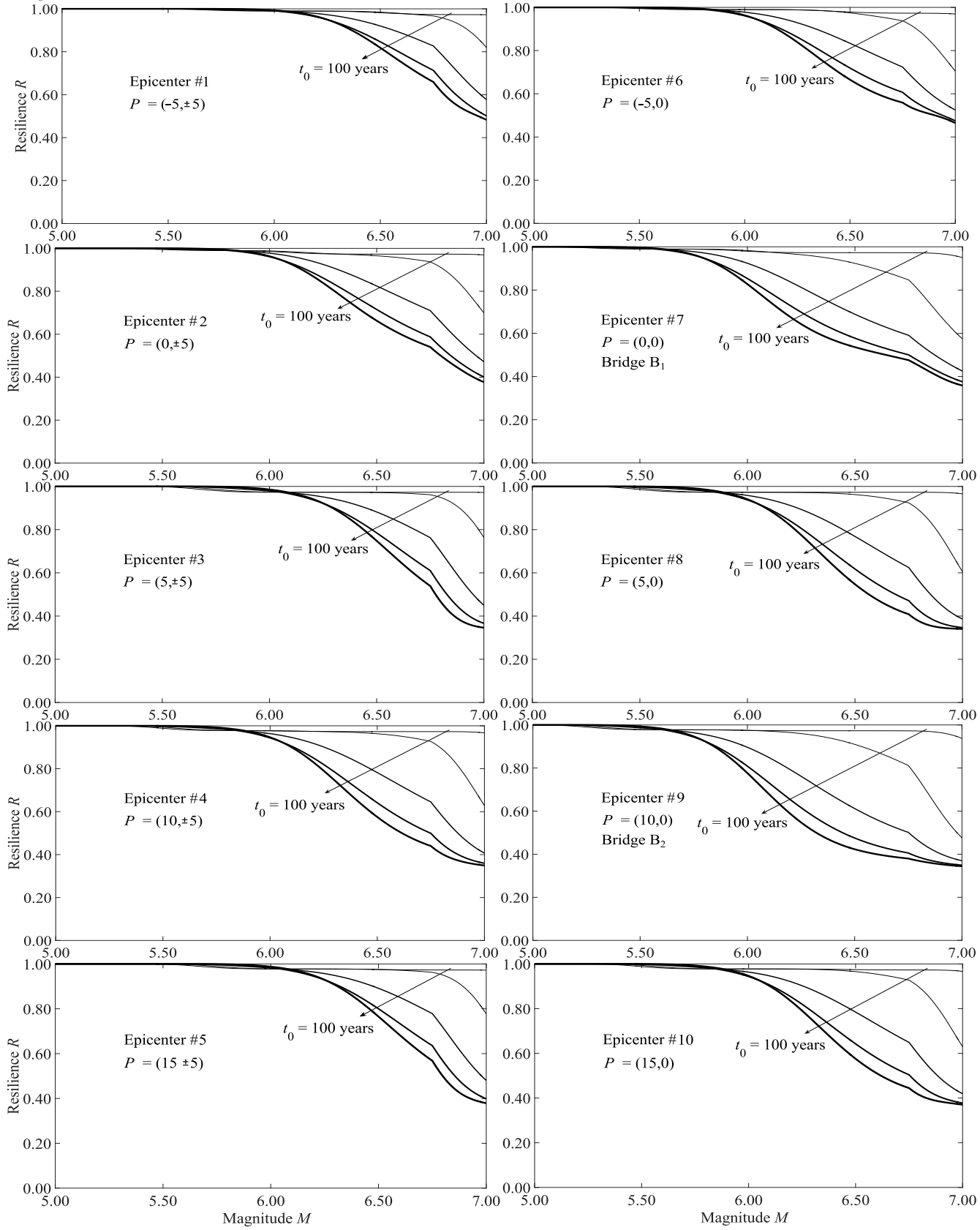

Fig. 7 – Seismic resilience of the highway network versus the earthquake magnitude for the set of epicenter locations shown in Fig. 6 (coordinates (x,y) in km, origin in the location of bridge B_1, epicenter #7) and different times of occurrence of the seismic event over a 100-year lifetime (t_0=0, 25, 50, 75, and 100 years).

5. Conclusions

A life-cycle probabilistic approach to seismic assessment of bridge structures and resilience analysis of road networks has been presented and applied to a highway network with RC bridges exposed to chloride-induced corrosion. A parametric analysis has been carried out by varying the moment magnitude and epicenter location to investigate the influence of the earthquake scenario and the role of road hierarchy and network structure. It has been found that the functionality of transportation networks can be substantially reduced due to seismic damage, in particular when severe traffic restrictions are applied to the most important bridges of the network. In addition, the effects of aging and structural deterioration can significantly reduce over time the seismic capacity of the bridges. Therefore, the combined effects of seismic and environmental hazards can exacerbate the loss of network functionality and make the seismic resilience depending on the time of occurrence of the seismic event. These detrimental effects can be partially mitigated by detours and re-entry links, or network upgrading with additional road branches aimed at increasing the minimum level of network resilience over the life-cycle.

The obtained results highlighted the important role of both the environmental exposure and earthquake scenario in a multi-hazard life-cycle-oriented approach to seismic design of resilient structures and infrastructures. Additional studies are required to investigate the correlation of the bridges in terms of environmental exposure, seismic capacities, damage states, and recovery processes, among others. Further research is also needed to account for the cumulative damage induced by multiple mainshocks or mainshock-aftershock sequences, as well as for the effects of other interacting natural hazards, including landslides and liquefactions.

6. References

[1] Chang SE (2009). Infrastructure resilience to disasters. *Frontiers of Engineering*, **39**(4), 36-41.

[2] Bocchini P, Frangopol DM (2011). A stochastic computational framework for the joint transportation network fragility analysis and traffic flow distribution under extreme events. *Probabilistic Engineering Mechanics*, **26**(2), 182-193.

[3] Bocchini P, Frangopol DM (2012). Optimal resilience- and cost-based post-disaster intervention prioritization for bridges along a highway segment. *Journal of Bridge Engineering*, ASCE, **17**(1), 117-129.

[4] Carturan F, Pellegrino C, Rossi R, Gastaldi M, Modena C (2013). An integrated procedure for management of bridge networks in seismic areas. *Bulletin of Earthquake Engineering*, **11**(2), 543-559.

[5] Muntasir Billah AHM, Shahria Alam M (2015). Seismic fragility assessment of highway bridges: a state-of-the-art review. *Structure and Infrastructure Engineering*, **11**(6), 804-832.

[6] Venkittaraman A, Banerjee S (2014). Enhancing resilience of highway bridges through seismic retrofit. *Earthquake Engineering and Structural Dynamics*, **43**(8), 1173-1191.

[7] Bruneau M, Chang SE, Eguchi RT, Lee GC, O'Rourke TD, Reinhorn AM, Shinozuka M, Tierney K, Wallace WA, Winterfeldt DV (2003). A framework to quantitatively assess and enhance the seismic resilience of communities. *Earthquake Spectra*, **19**(4), 733-752.

[8] Cimellaro, G.P., Reinhorn, A.M. & Bruneau, M. (2010). Framework for analytical quantification of disaster resilience. *Engineering Structures*, **32**(11), 3639-3649.

[9] Bocchini P, Decò A, Frangopol DM (2012). Probabilistic functionality recovery model for resilience analysis. *6th International Conference on Bridge Maintenance, Safety and Management* (IABMAS 2012), Stresa, Italy, July 8-12. In: *Bridge Maintenance, Safety, Management, Resilience and Sustainability*, F. Biondini & D.M. Frangopol (Eds.), CRC Press/Balkema, Taylor & Francis Group, London, UK.

[10] Decò A, Bocchini P, Frangopol DM (2013). A probabilistic approach for the prediction of seismic resilience of bridges. *Earthquake Engineering and Structural Dynamics*, **42**(10), 1469-1487.

[11] Chang SE, Shinozuka M (2004). Measuring improvements in the disaster resilience of communities. *Earthquake Spectra*, **20**(3), 739-755.

[12] Bruneau M, Reinhorn AM (2007). Exploring the concept of seismic resilience for acute care facilities. *Earthquake Spectra*, **23**(1), 41-62.

[13] Biondini F, Capacci L, Titi A (2015). Seismic resilience of bridges and highway networks. *16th Congress of the Italian Association of Earthquake Engineering* (ANIDIS 2015), L'Aquila, Italy, September 13-17, 2015.

[14] Titi A, Biondini F (2013). Resilience of concrete frame structures under corrosion. *11th International Conference on Structural, Safety & Reliability* (ICOSSAR 2013), New York, NY, USA, June 16-20. In: *Safety, Reliability, Risk and*

Life-Cycle Performance of Structures and Infrastructures, G. Deodatis, B.R. Ellingwood & D.M. Frangopol (Eds.), CRC Press/Balkema, Taylor & Francis Group, London, UK.

[15] Biondini F, Camnasio E, Titi A (2015). Seismic resilience of concrete structures under corrosion. *Earthquake Engineering and Structural Dynamics*, **44**(14), 2445-2466.

[16] Titi A, Biondini F, Frangopol DM (2015). Seismic resilience of deteriorating concrete structures, *Proceedings of the ASCE Structures Congress*, Portland, OR, USA, April 22-25, 2015. In: *Structures Congress 2015*, N. Ingraffea & M. Libby (Eds.), ASCE, CD-ROM, 1649-1660.

[17] Vamvatsikos D, Cornell CA (2002). Incremental dynamic analysis. *Earthquake Engineering and Structural Dynamics*, **31**(3), 491-514.

[18] Biondini F, Camnasio E, Palermo A (2014). Lifetime seismic performance of concrete bridges exposed to corrosion. *Structure and Infrastructure Engineering*, **10**(7), 880-900.

[19] Mander J, Priestley MJN, Park R (1988). Theoretical stress-strain model for confined concrete. *Journal of Structural Engineering*, **114**(8), 1804-1826.

[20] Takeda T, Sozen MA, Nielsen NN (1970). Reinforced concrete response to simulated earthquake. *Journal of the Structural Division*, ASCE, **11**(2), 10-21.

[21] Paulay T, Priestley MJN (1992). *Seismic design of reinforced concrete and masonry structures*, John Wiley & Sons, Hoboken, NJ, USA.

[22] Capacci L (2015). *Seismic resilience of bridge networks*. Master Thesis, Politecnico di Milano, Milan, Italy.

[23] Bertolini L, Elsener B, Pedeferri P, Polder R (2004). *Corrosion of steel in concrete*. Wiley-VCH, Weinheim, Germany.

[24] Biondini F, Bontempi F, Frangopol DM, Malerba PG (2004). Cellular automata approach to durability analysis of concrete structures in aggressive environments. *Journal of Structural Engineering*, ASCE, **130**(11), 1724-1737.

[25] Biondini F, Bontempi F, Frangopol DM, Malerba PG (2006). Probabilistic service life assessment and maintenance planning of concrete structures. *Journal of Structural Engineering*, ASCE, **132**(5), 810-825.

[26] Biondini F, Vergani M (2015). Deteriorating beam finite element for nonlinear analysis of concrete structures under corrosion. *Structure and Infrastructure Engineering*, **11**(4), 519-532.

[27] Bindi D, Pacor F, Luzi L, Puglia R, Massa M, Ameri G, Paolucci R (2011). Ground motion prediction equations derived from the Italian strong motion database. *Bulletin of Earthquake Engineering*, **9**(6), 1899-1920.

[28] Martin WA, McGuckin NA (1998). *Travel estimation techniques for urban planning*. NCHRP Report 365, Transportation Research Board, TRB, Washington, DC, USA.

[29] Erath A, Birdsall J, Axhausen KW, Hajdin R (2009). Vulnerability assessment methodology for Swiss road network. *Journal of the Transportation Research Board*, 2137, 118–126, TRB, Washington, DC, USA.

[30] Mackie KR, Stojadinović B (2006). Post-earthquake functionality of highway overpass bridges. *Earthquake Engineering and Structural Dynamics*, **35**(1), 77-93.

[31] Biondini F, Frangopol DM, Garavaglia E (2008). Life-cycle reliability analysis and selective maintenance of deteriorating structures. *4th International Conference on Bridge Maintenance, Safety and Management* (IABMAS 2008), Seoul, Korea, July 13-17, 2008. In: *Bridge Maintenance, Safety, Management, Health Monitoring and Informatics*, H-M. Koh & D.M. Frangopol (Eds.), CRC Press/Balkema, Taylor & Francis, London, UK.

[32] Padgett JE, DesRoches R (2007). Bridge functionality relationships for improved seismic risk assessment of transportation networks. *Earthquake Spectra*, **23**(1), 115-130.

[33] Pinto AV, Verzeletti G, Magonette G, Pegon P, Negro P, Guedes J (1996). Pseudo-dynamic testing of large-scale R/C bridges in ELSA. *11th World Conference on Earthquake Engineering*, Acapulco, Mexico, June 23-28.

[34] Ni P, Petrini L, Paolucci R (2014). Direct displacement-based assessment with nonlinear soil-structure interaction for multi-span reinforced concrete bridges. *Structure and Infrastructure Engineering*, **10**(9), 1211-1227.

[35] Mander JB, Dhakal RP, Mashiko N, Solberg KM (2007). Incremental dynamic analysis applied to seismic financial risk assessment of bridges. *Engineering Structures*, **29**(10), 2662-2672.

[36] SIMQKE (1976). *A program for artificial ground motion generation*. User's Manual and Documentation, NISEE, Massachusetts Institute of Technology, MA, USA.

[37] CEN-EN 1998-1 (2004). *Eurocode 8: Design of structures for earthquake resistance – Part 1: General rules, seismic actions and rules for buildings*. European Committee for Standardization, Brussels, Belgium.

[38] Dolšek M (2009). Incremental dynamic analysis with consideration of modeling uncertainties. *Earthquake Engineering and Structural Dynamics*, **38**(6), 805-825.